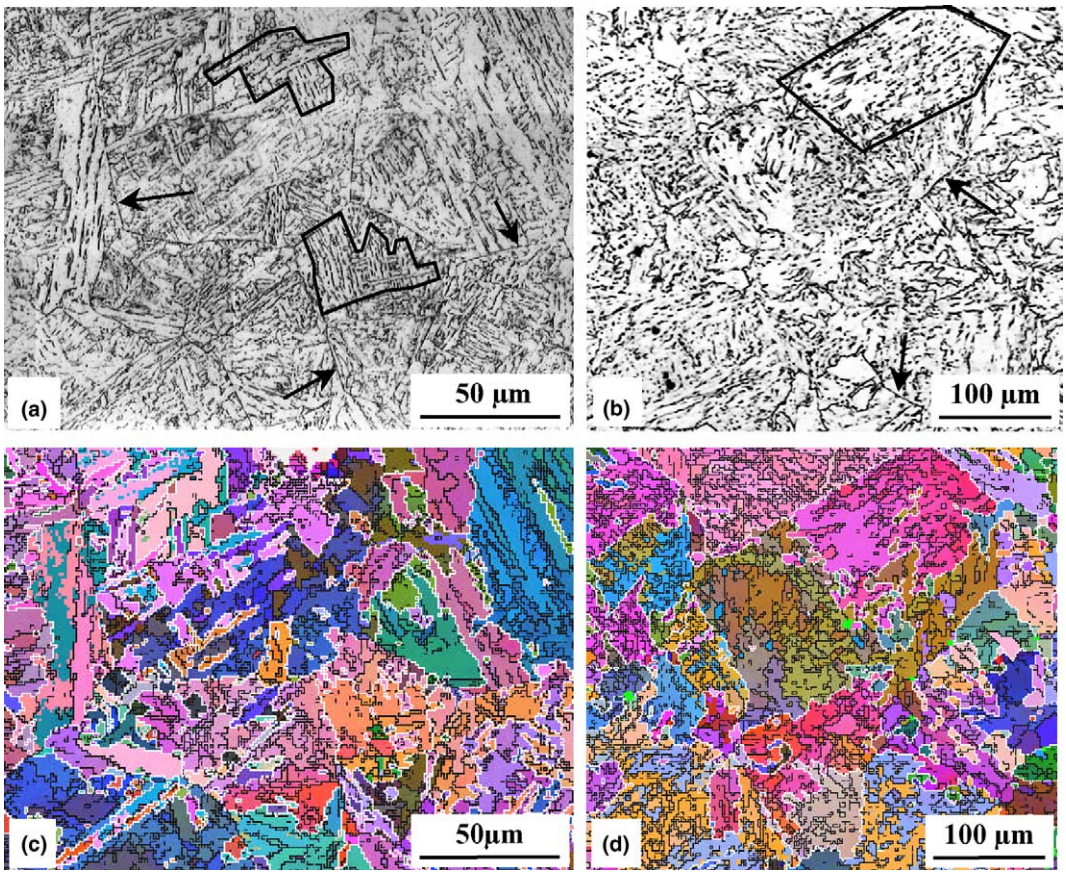

Fig. 4. Light optical micrographs obtained after (a) MI and (b) HI thermal cycles (nital etching). Corresponding EBSD maps are shown in (c) and (d), respectively, with a colour key according to the local orientation (one colour for each of the three Euler angles). Thin white and black lines indicate misorientation angles greater and lower than 20°, respectively. Morphological packets and former austenite grain boundaries are indicated with thick black lines and arrows, respectively.

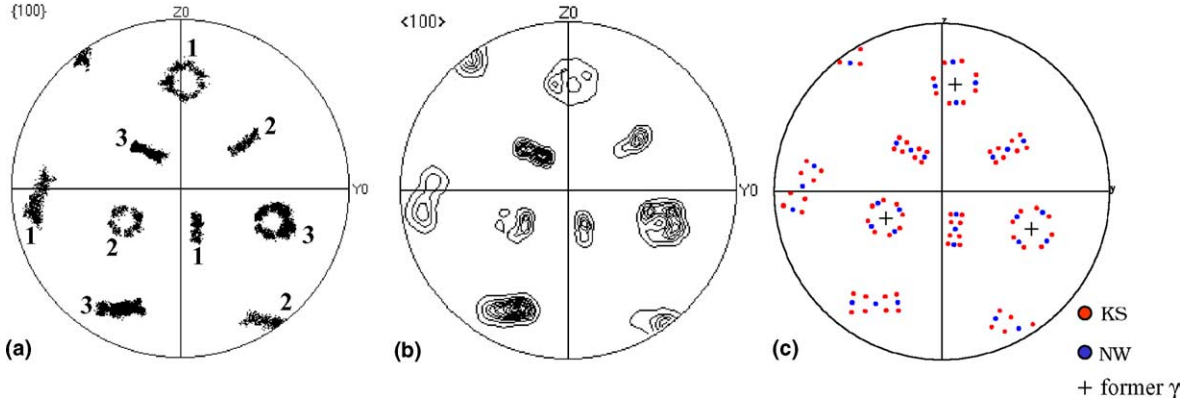

Fig. 5. $\{001\}_{\alpha}$ Pole figures from a former austenite grain in the MI microstructure. (a) Discrete and (b) density pole figure plots. (c) Orientations of the KS and NW variants calculated from the same former austenite grain. Numbers refer to the three Bain zones of the austenite phase.

3.3.2. Orientation relationships between bainite packets

The crystallographic relationships between neighbouring variants, which control cleavage microcrack propagation, were also investigated. Fig. 6(a) shows typical histograms of misorientation angle between neighbouring bainite crystals within a single former austenite grain. Obviously, only certain misorientation angles are found. These histograms were compared with theoretical histograms calculated using KS or NW orientation relationships and assuming that all pairs of neighbouring variants had the same probability to be found [7] (Fig. 6(b)). Comparison of Fig. 6(a) with 6(b)